The role of cluster mass in the multiple populations of Galactic and extragalactic Globular Clusters

Lagioia E. P. et al. 2019

Astronomical Journal, 158:202

Interpretation: Mixing or Primordial Abundance Variations?

EVIDENCE FOR MIXING It is hard to avoid the conclusion that globular cluster giants mix the ashes of internal nuclear processing to the surface on a scale larger than expected on the basis of classical evolutionary theory. The existence of CH and Ba stars in late evolutionary stages in clusters in

which the vast majority of stars show no *generally* strong enhancement of carbon or s-process species suggests the correctness of the mixing hypothesis. CH stars seem to require that carbon produced by triple-α processing be mixed to the surface either at the He-core or shell flashes and the presence of Ba-stars in clusters suggests that the convective linkage necessary to operate the neutron-source chain $^{12}C(p,\gamma)^{13}N(\beta^+\nu)^{13}C(\alpha,n)^{16}O$ in low mass stars must indeed exist.

In typical metal-poor cluster stars, as early as the mid-SGB, the average carbon abundance begins to decline presumably in response to the processing of the base of the convective envelope through the CN cycle, and continues to drop to $\sim$0.1 of the original value, or lower, with advancing evolutionary state. The onset of the decline thus occurs much earlier and the magnitude of the effect is much larger than we would have expected based on the degree of CN processing and mixing found in conventional evolutionary models. Unfortunately, even with the improved observational technology cited earlier, it is not yet possible to recover the expected changes in the $^{12}C/^{13}C$ ratio in these stars. The lack of anti-

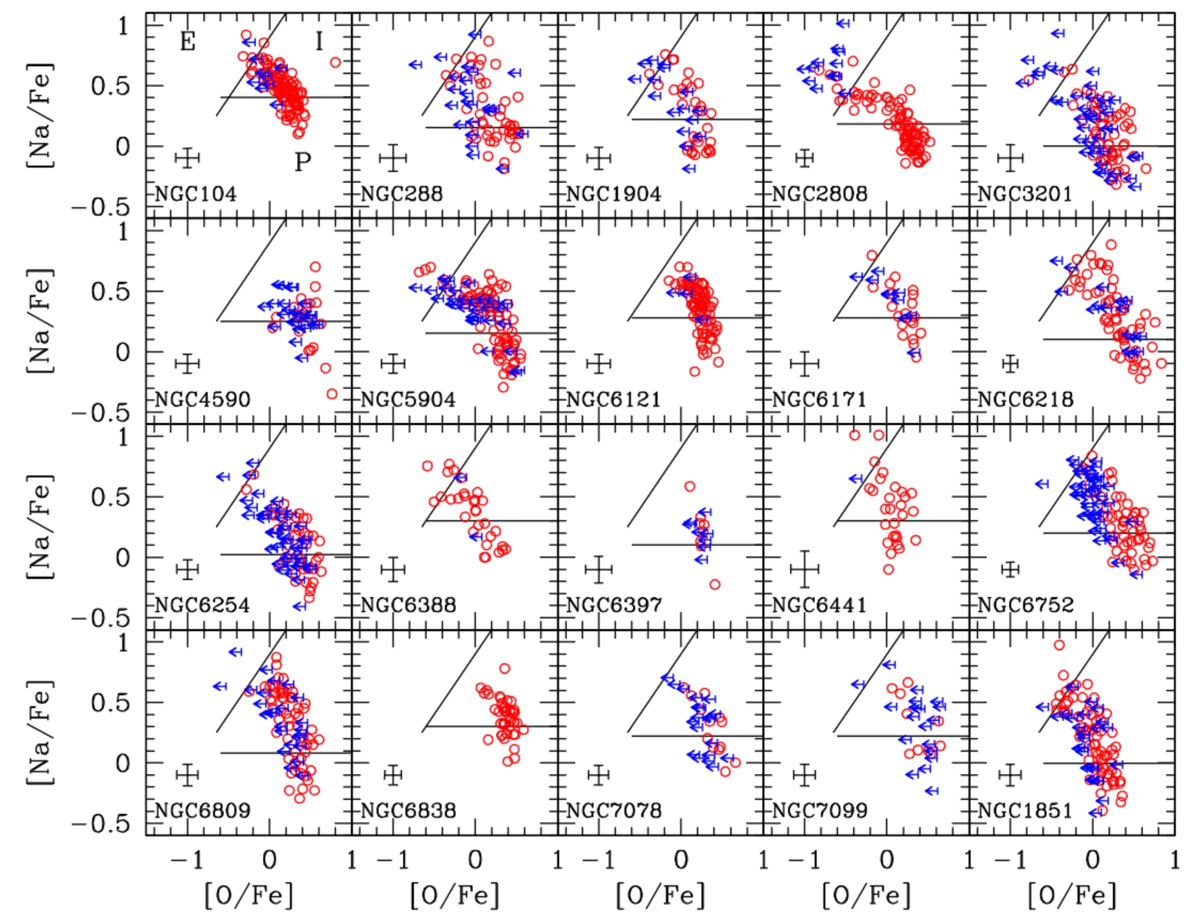

Fig. 2 A modern collection of Na-O anticorrelations showing partial results of the FLAMES survey of globular clusters (see Carretta et al. 2009a, 2010d for full references) and demonstrating both the ubiquity of this feature and its difference cluster-to-cluster. The lines separate the P (first generation), I, and E (second generation) components, as defined in Carretta et al. In this plot, red circles are measures for both O and Na, and blue arrows are measures for Na but only upper limits for O.

Kraft 1979

Gratton+ 2012

The "second"

parameter

of

HBs

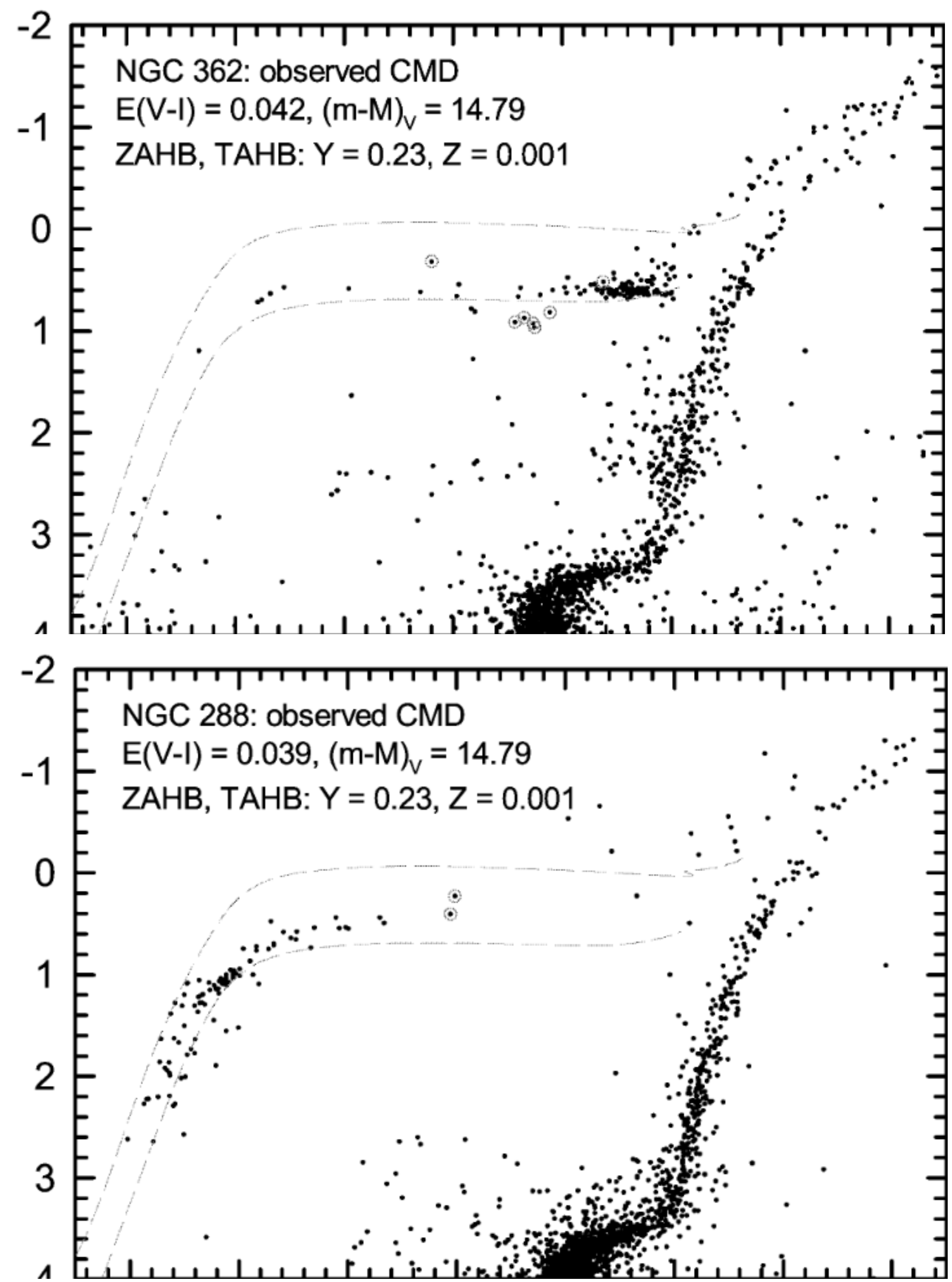

Catelan+ 2001

Piotto+ 2007

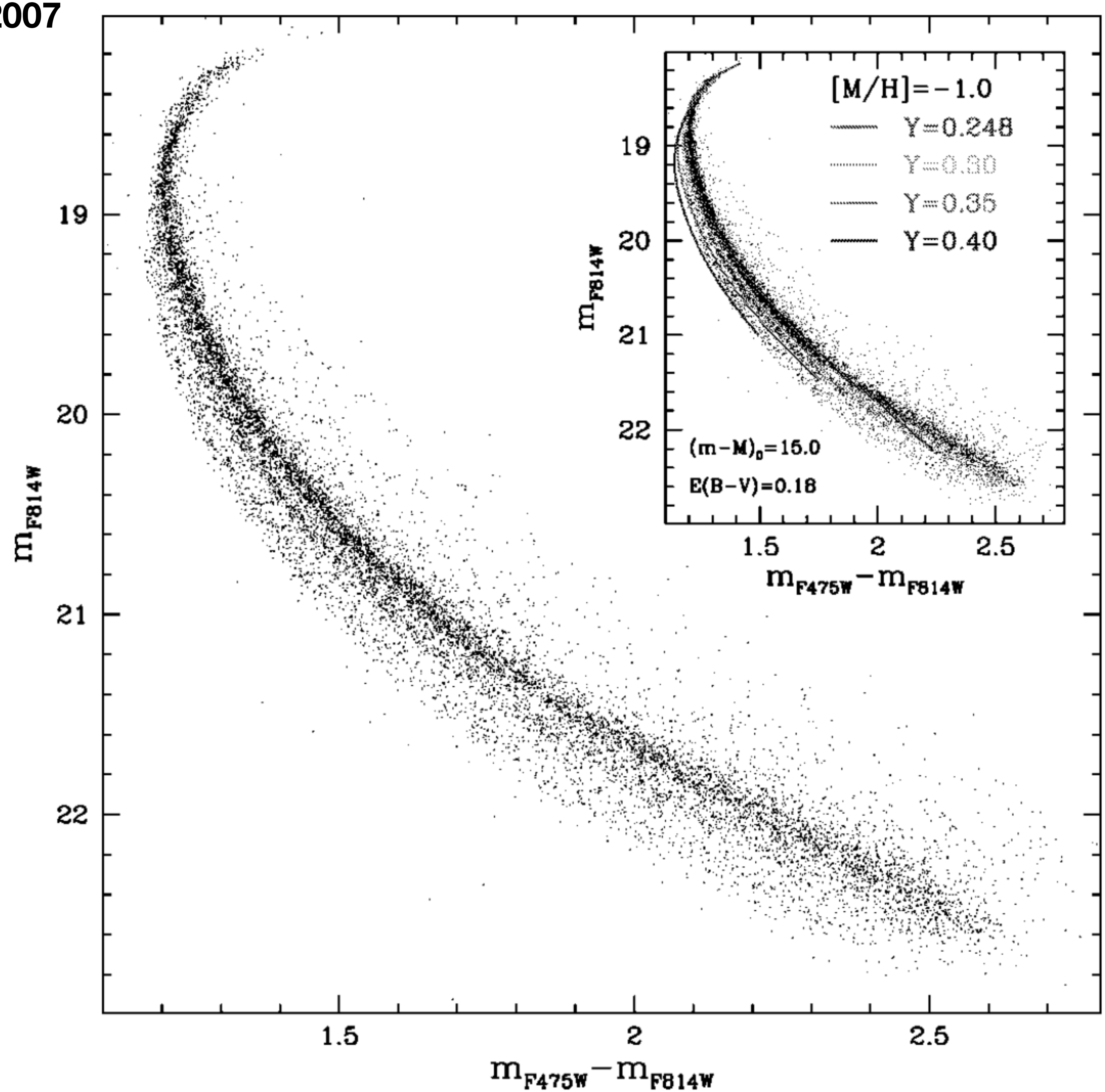

19
20
21
22
m_{F814W}
1.5
2
2.5
$m_{F475W}-m_{F814W}$
[M/H]=-1.0
Y=0.248
Y=0.30
Y=0.35
Y=0.40
(m-M)$_0$=15.0
E(B-V)=0.18

Milone+ 2012

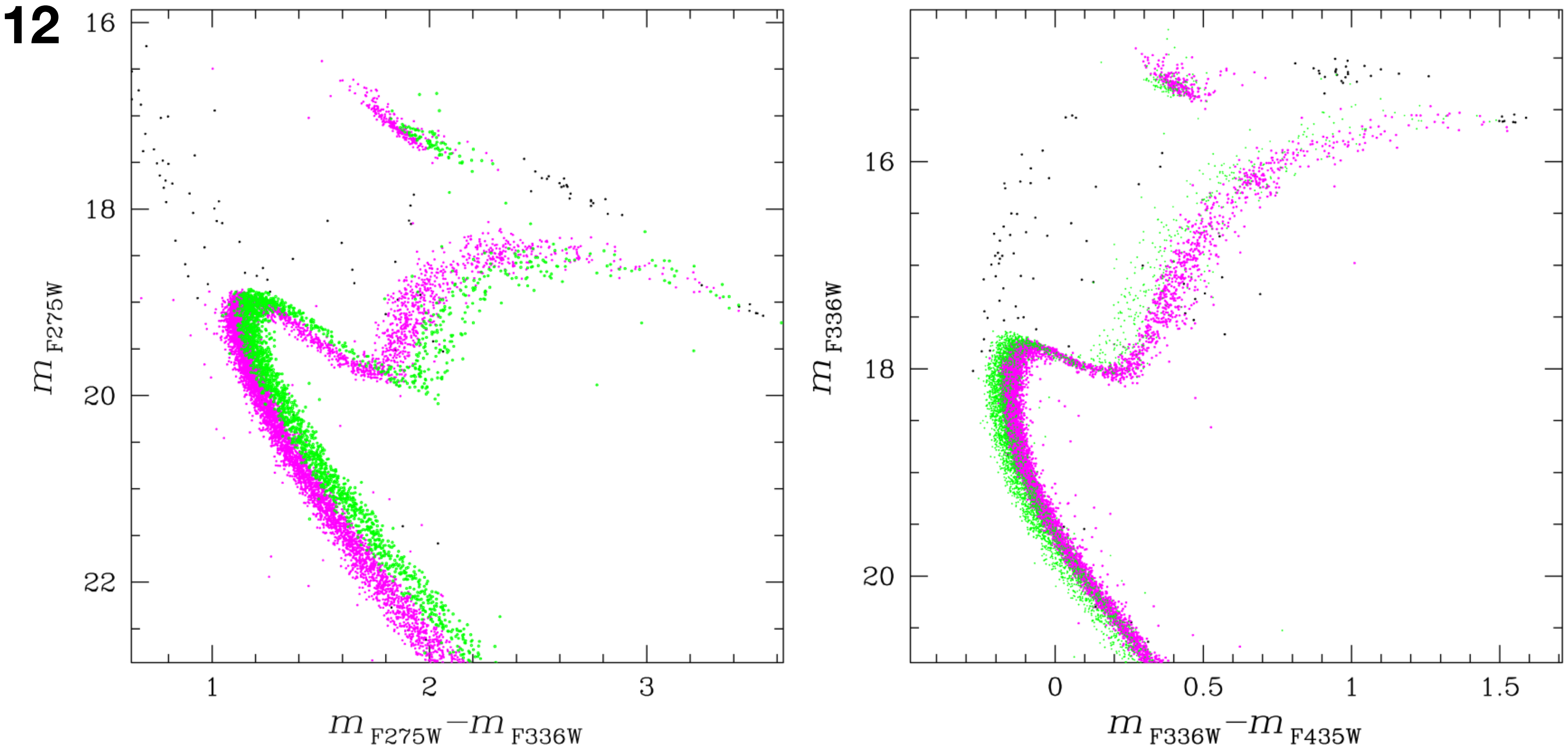

Figure 35. CMDs with m_{F275W} vs. $m_{F275W} - m_{F336W}$ (left) and m_{F336W} vs. $m_{F336W} - m_{F435W}$ (right). We have colored in green and magenta the two groups of stars selected in Figure 34. This is the first time anyone has been able to follow two stellar populations in a GC from the main sequence to the HB.

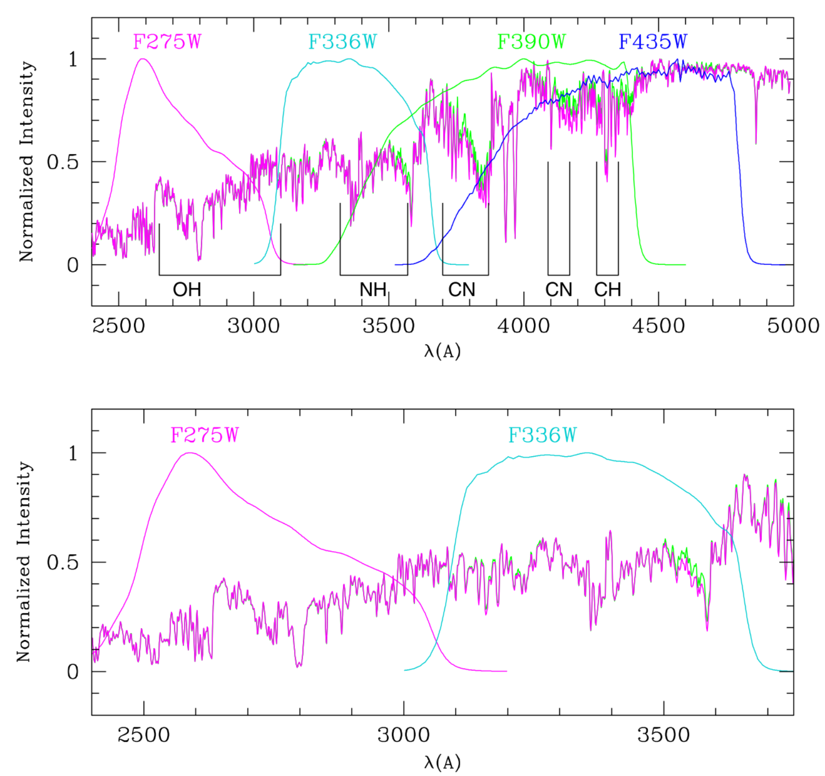

Figure 32. Top panel: comparison between two synthetic spectra: one for an N-rich star (magenta) and one for an N-poor star (black). The spectra are given as flux (in arbitrary units) and are smoothed at 1 Å resolution for clarity; they have been computed for parameters typical of a subgiant star in 47 Tuc, with chemical compositions given in the text. For reference, the normalized throughputs of the bluest broadband filters of WFC3/UVIS F(275/336/390/435/475)W are also shown. Labels on the bottom indicate the wavelength range where important spectroscopic features involving CNO elements cause significant absorption. The most important contributions come from OH at ∼2600–3100 Å and NH at ∼3300–3600 Å. Bottom panel: a zoom-in of the spectral region that is of particular interest for the present paper.

CNO variations mapped

through a specific combination

of UV and optical/NIR bands

Milone+ 2017

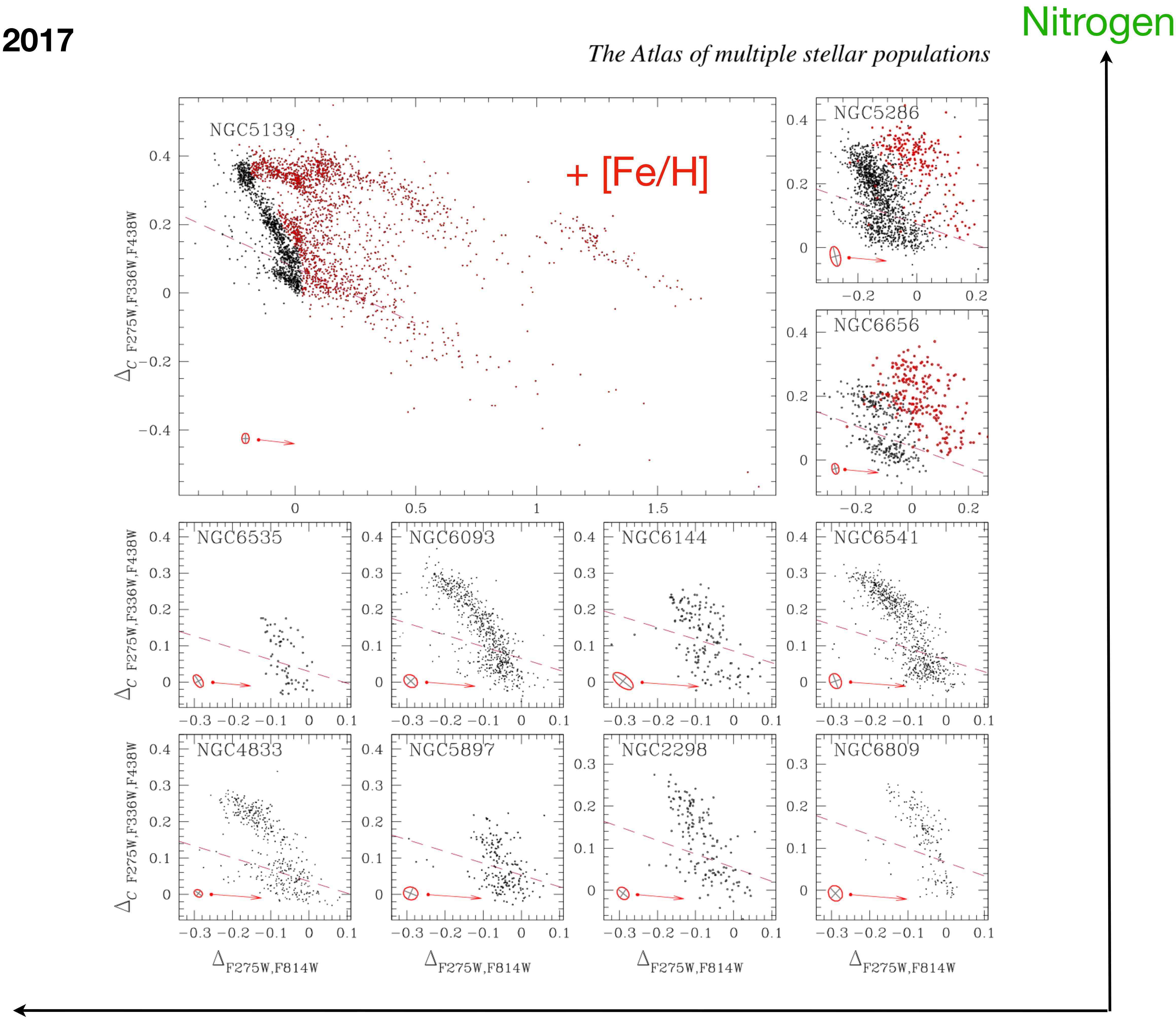

Nitrogen
The Atlas of multiple stellar populations
NGC5139
+ [Fe/H]
NGC5286
NGC6656
NGC6535
NGC6093
NGC6144
NGC6541
NGC4833
NGC5897
NGC2298
NGC6809
$\Delta_{C\ F275W,F336W,F438W}$
$\Delta_{F275W,F814W}$
Helium

Type II GCs

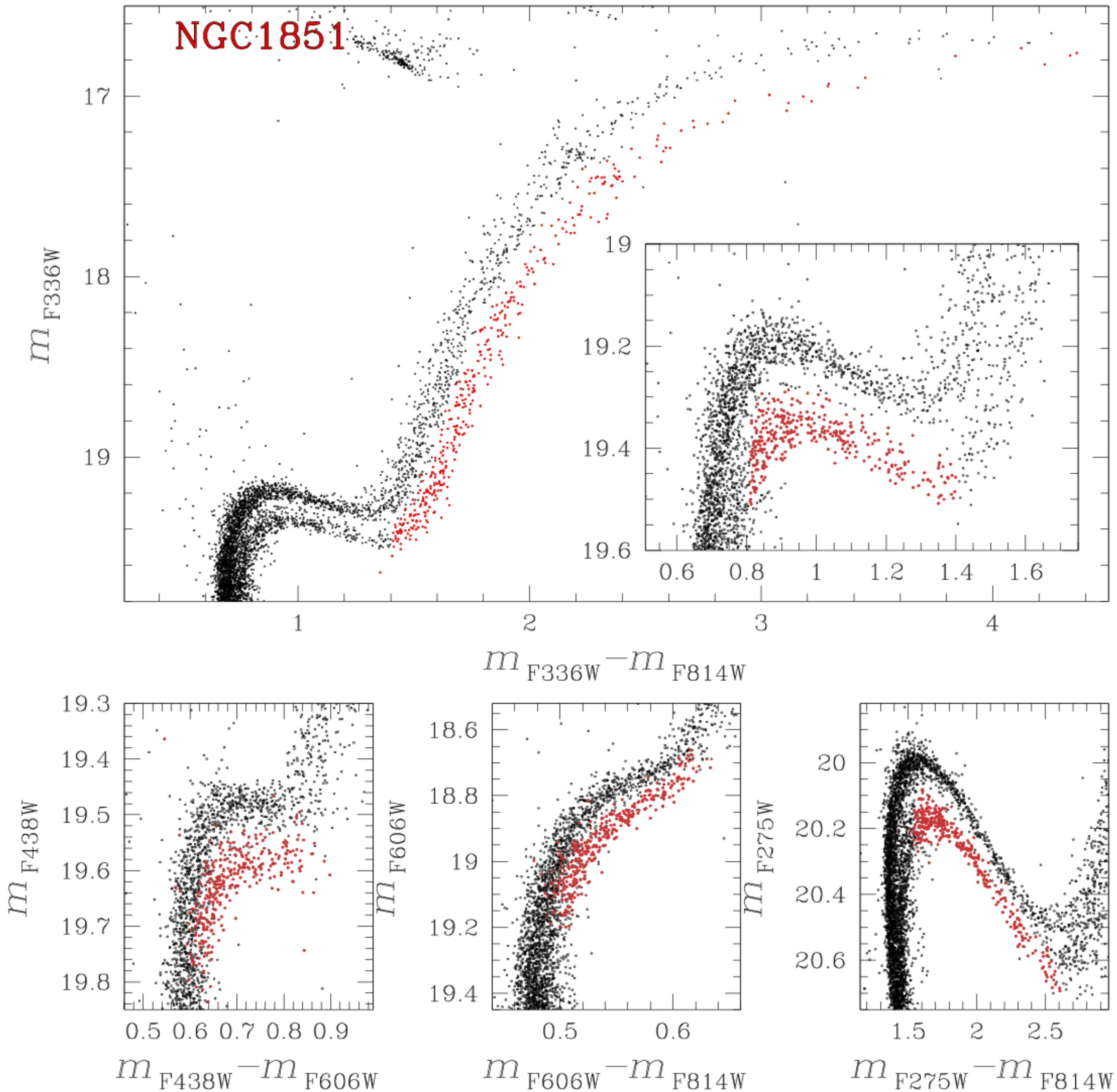

Milone+ 2017

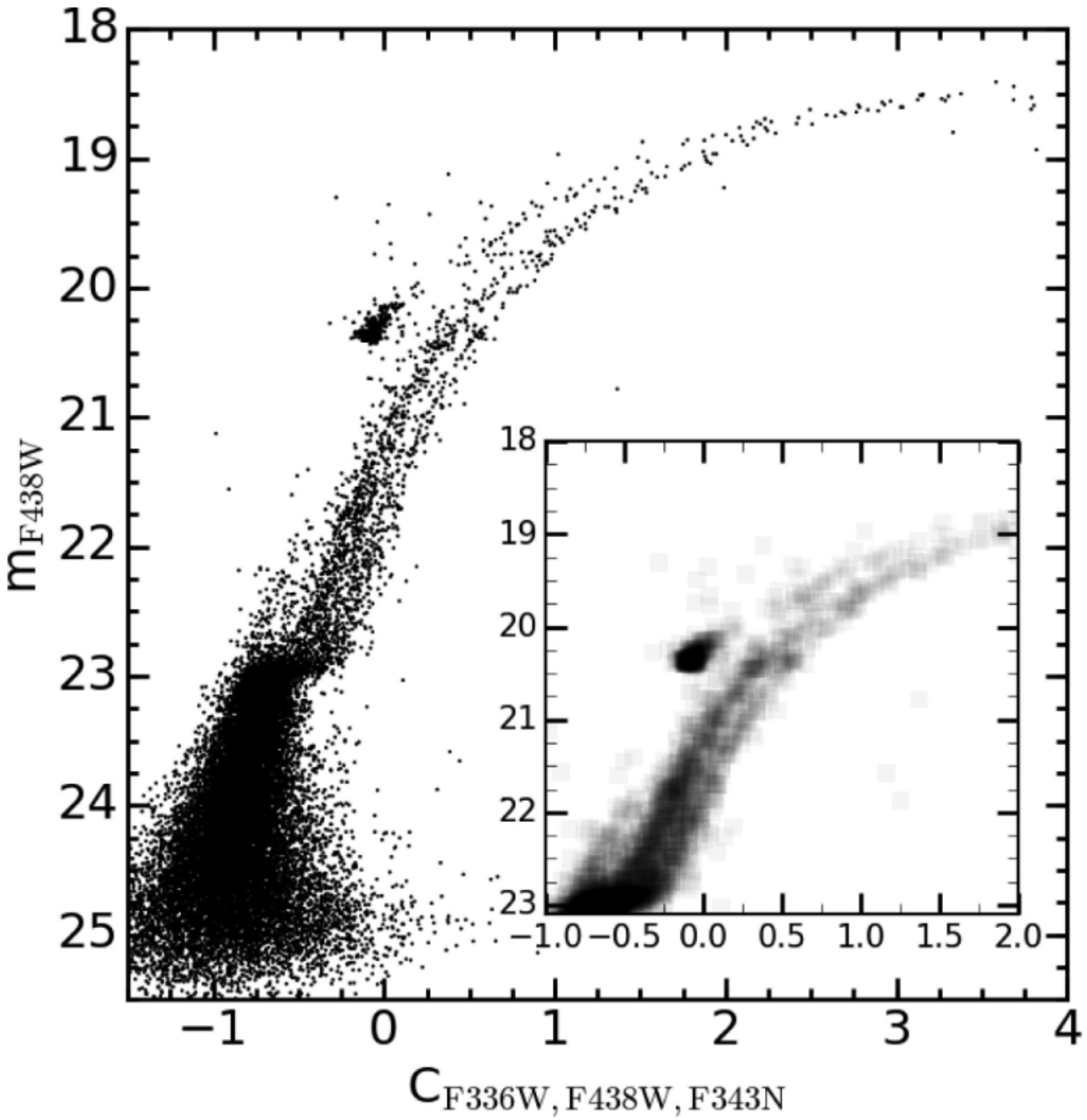

Niederhofer+ 2017

Old globular clusters

in the Magellanic clouds

also contain MSPs

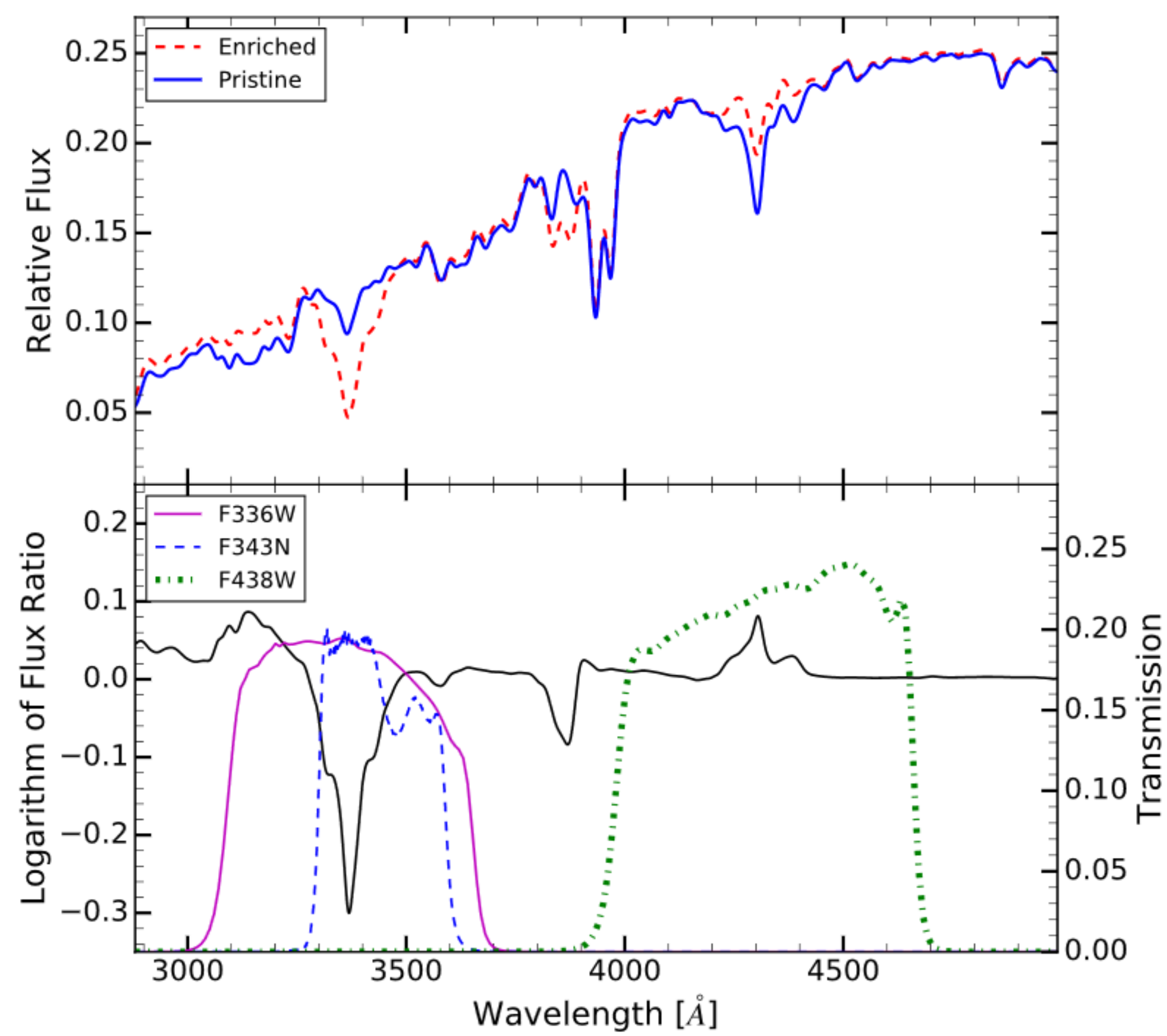

MSPs with ground-based photometry

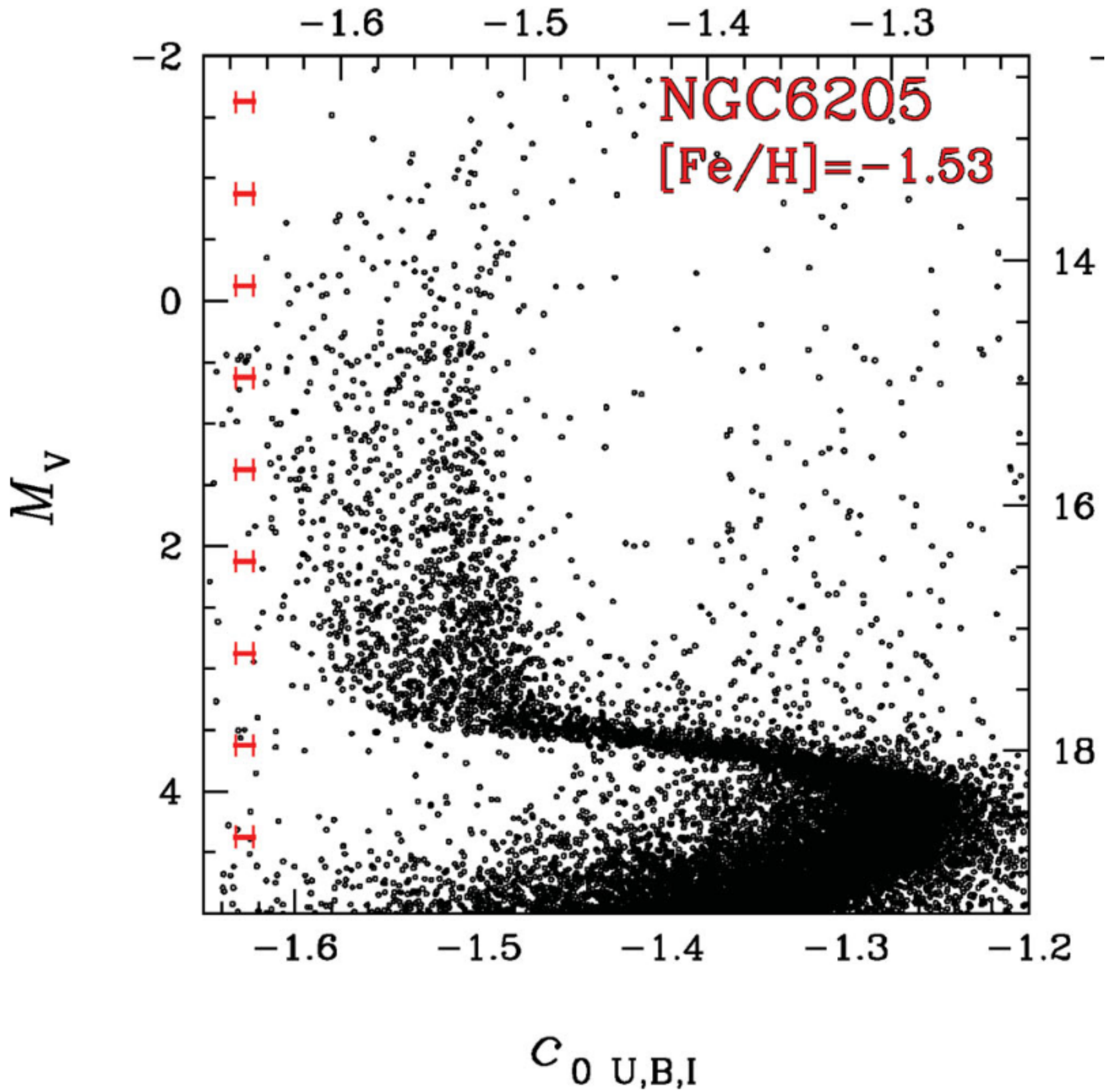

Monelli+ 2013

The RGB width

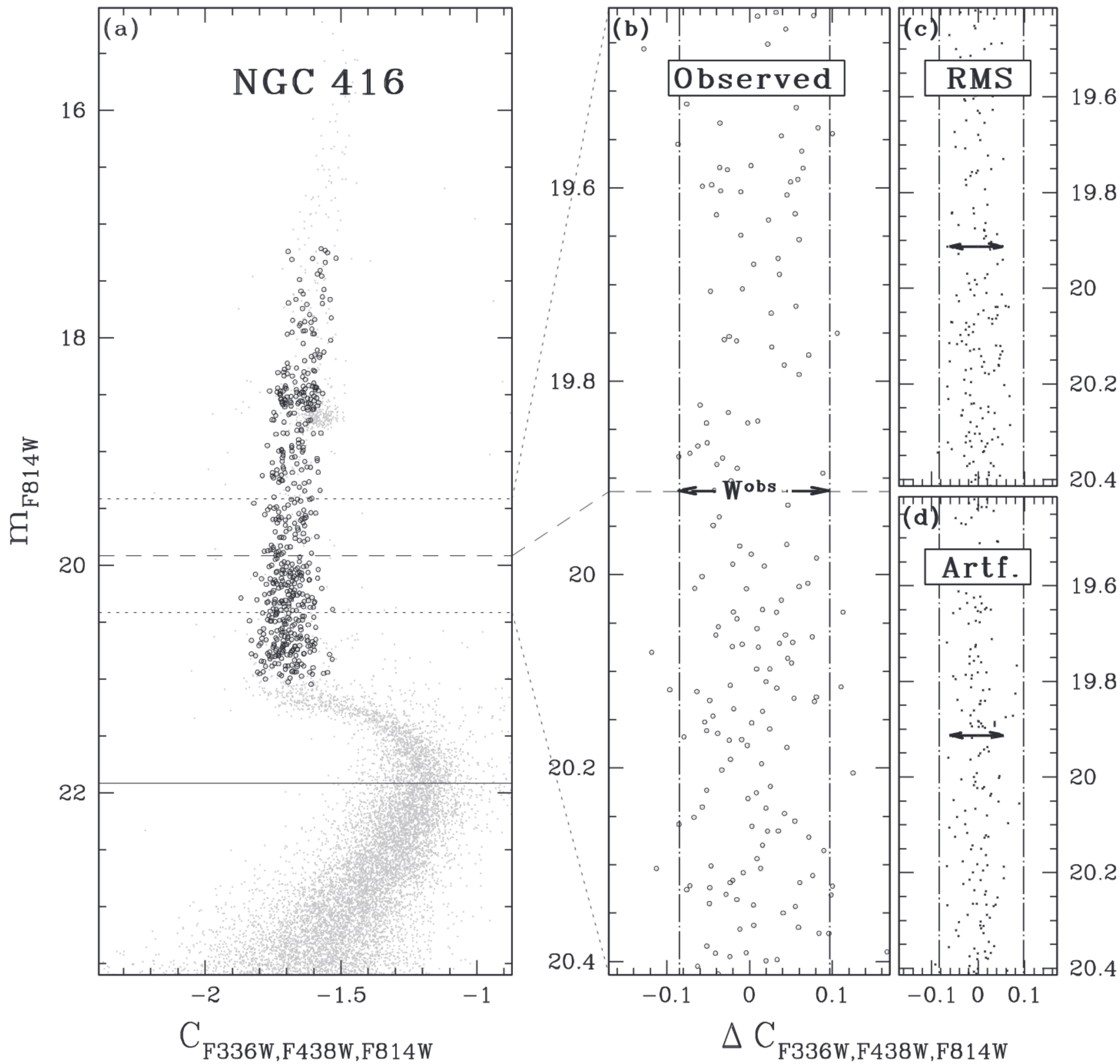

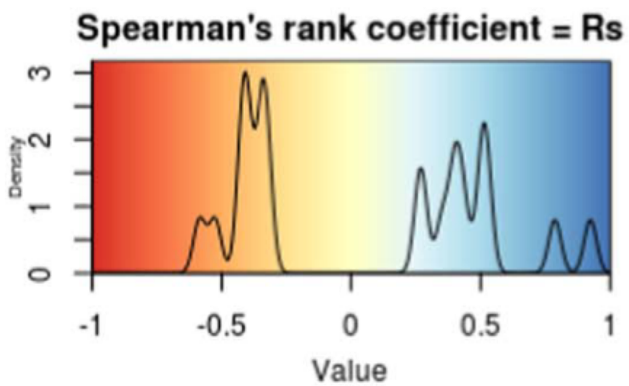

Correlation map of RGB Width against 45 GC parameters

[Fe/H] 0.787 (56) <0.01	epsilon -0.038 (54) 0.78	r_hl -0.245 (56) 0.06	T_rh -0.092 (56) 0.49	eta_c -0.123 (56) 0.36	Z -0.131 (56) 0.33	R_perig -0.204 (56) 0.12	<dY> 0.197 (55) 0.14	F_bin(c) 0.108 (34) 0.53
E(B-V) 0.352 (56) 0.01	c 0.172 (56) 0.20	r_hm -0.337 (56) 0.01	MF slope 0.266 (56) 0.04	eta_hm 0.172 (56) 0.20	U 0.055 (56) 0.68	R_apog -0.322 (56) 0.01	dY_max 0.436 (55) <0.01	F_bin(hm) -0.135 (45) 0.36
Mv -0.420 (56) <0.01	Mass 0.397 (56) <0.01	r_t -0.017 (56) 0.90	F_remn 0.231 (56) 0.08	<RV> 0.005 (56) 0.97	V 0.079 (56) 0.55	age_MF09 -0.071 (54) 0.60	W_C (M17) 0.924 (56) <0.01	F_bin(o-hm) -0.335 (41) 0.03
SB_0 -0.411 (56) <0.01	M/L -0.040 (56) 0.77	rho_c 0.273 (56) 0.04	sigma_0 0.513 (56) <0.01	X -0.197 (56) 0.14	W -0.073 (56) 0.58	age_D10 -0.395 (56) <0.01	N_1G/N_tot -0.416 (52) <0.01	HBR -0.586 (55) <0.01
rho_0 0.408 (56) <0.01	r_c -0.180 (56) 0.18	rho_hm 0.525 (56) <0.01	v_esc 0.505 (56) <0.01	Y -0.150 (56) 0.26	R_GC -0.354 (56) 0.01	age_V13 -0.526 (49) <0.01	S(RR Lyr) -0.192 (55) 0.15	L2 0.181 (55) 0.18

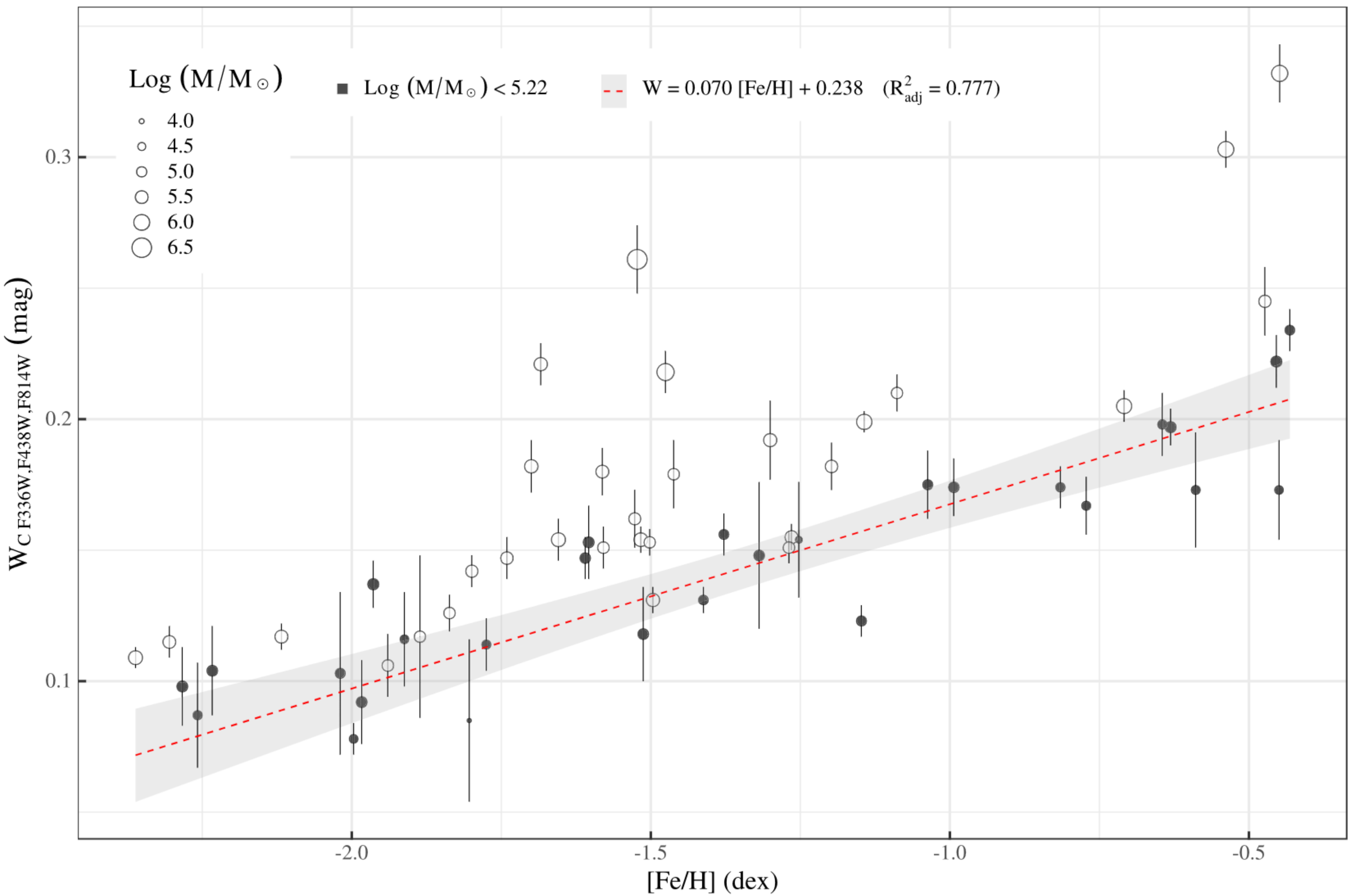

Log (M/M☉)
4.0
4.5
5.0
5.5
6.0
6.5
Log (M/M☉) < 5.22
W = 0.070 [Fe/H] + 0.238 (R^2_{adj} = 0.777)
0.1
0.2
0.3
$W_{C\ F336W,F438W,F814W}$ (mag)
-2.0
-1.5
-1.0
-0.5
[Fe/H] (dex)

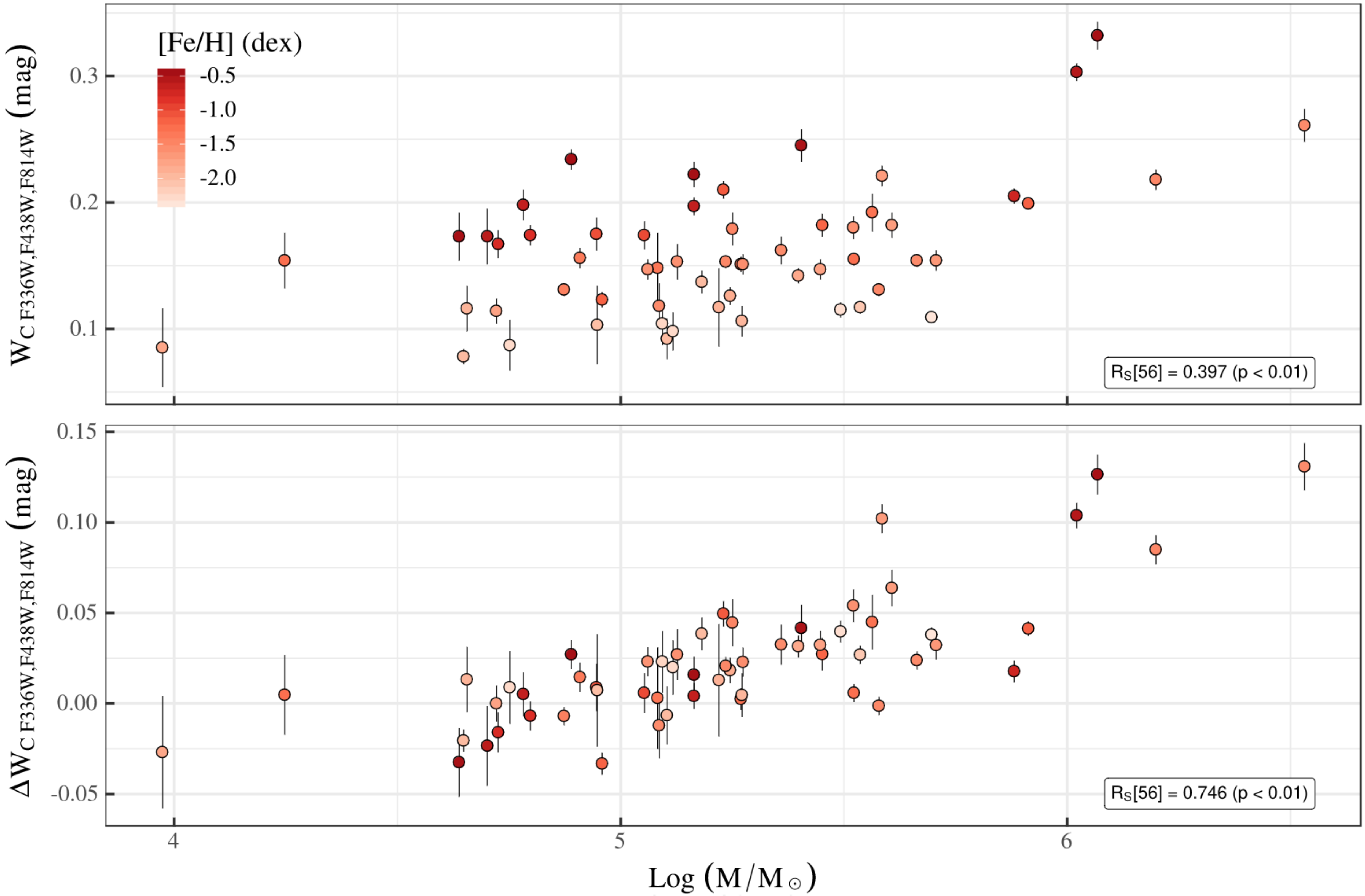
[Fe/H] (dex)
-0.5
-1.0
-1.5
-2.0
$W_{C\ F336W,F438W,F814W}$ (mag)
$R_S[56] = 0.397$ ($p < 0.01$)
$\Delta W_{C\ F336W,F438W,F814W}$ (mag)
$R_S[56] = 0.746$ ($p < 0.01$)
Log $(M/M_\odot)$

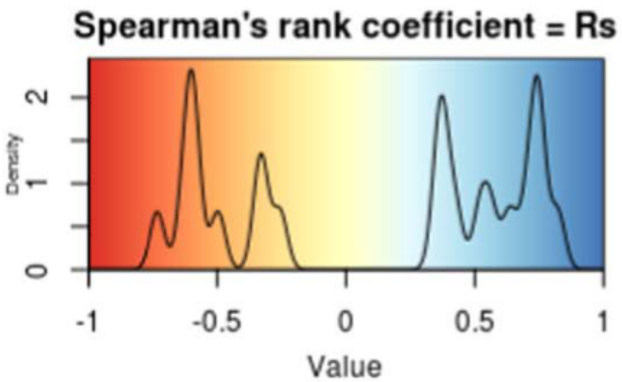

Correlation map
of
'normalized' RGB Width against 44 GC parameters

	epsilon -0.020 (54) 0.88	r_hl -0.334 (56) 0.01	T_rh 0.162 (56) 0.22	eta_c -0.256 (56) 0.05	Z 0.082 (56) 0.54	R_perig -0.137 (56) 0.30	<dY> 0.357 (55) 0.01	F_bin(c) -0.497 (34) <0.01
E(B-V) 0.080 (56) 0.55	c 0.376 (56) <0.01	r_hm -0.327 (56) 0.01	MF slope -0.220 (56) 0.10	eta_hm 0.047 (56) 0.72	U -0.096 (56) 0.48	R_apog -0.006 (56) 0.96	dY_max 0.703 (55) <0.01	F_bin(hm) -0.589 (45) <0.01
Mv -0.733 (56) <0.01	Mass 0.746 (56) <0.01	r_t 0.372 (56) <0.01	F_remn -0.183 (56) 0.17	<RV> 0.059 (56) 0.66	V 0.070 (56) 0.60	age_MF09 -0.191 (54) 0.16	DW_C (M17) 0.822 (56) <0.01	F_bin(o-hm) -0.628 (41) <0.01
SB_0 -0.606 (56) <0.01	M/L 0.027 (56) 0.84	rho_c 0.426 (56) <0.01	sigma_0 0.749 (56) <0.01	X -0.094 (56) 0.48	W -0.126 (56) 0.35	age_D10 0.079 (56) 0.56	N_1G/N_tot -0.591 (52) <0.01	HBR 0.044 (55) 0.74
rho_0 0.520 (56) <0.01	r_c -0.232 (56) 0.08	rho_hm 0.636 (56) <0.01	v_esc 0.743 (56) <0.01	Y -0.054 (56) 0.69	R_GC -0.026 (56) 0.85	age_V13 0.182 (49) 0.20	S(RR Lyr) 0.062 (55) 0.65	L2 0.562 (55) <0.01

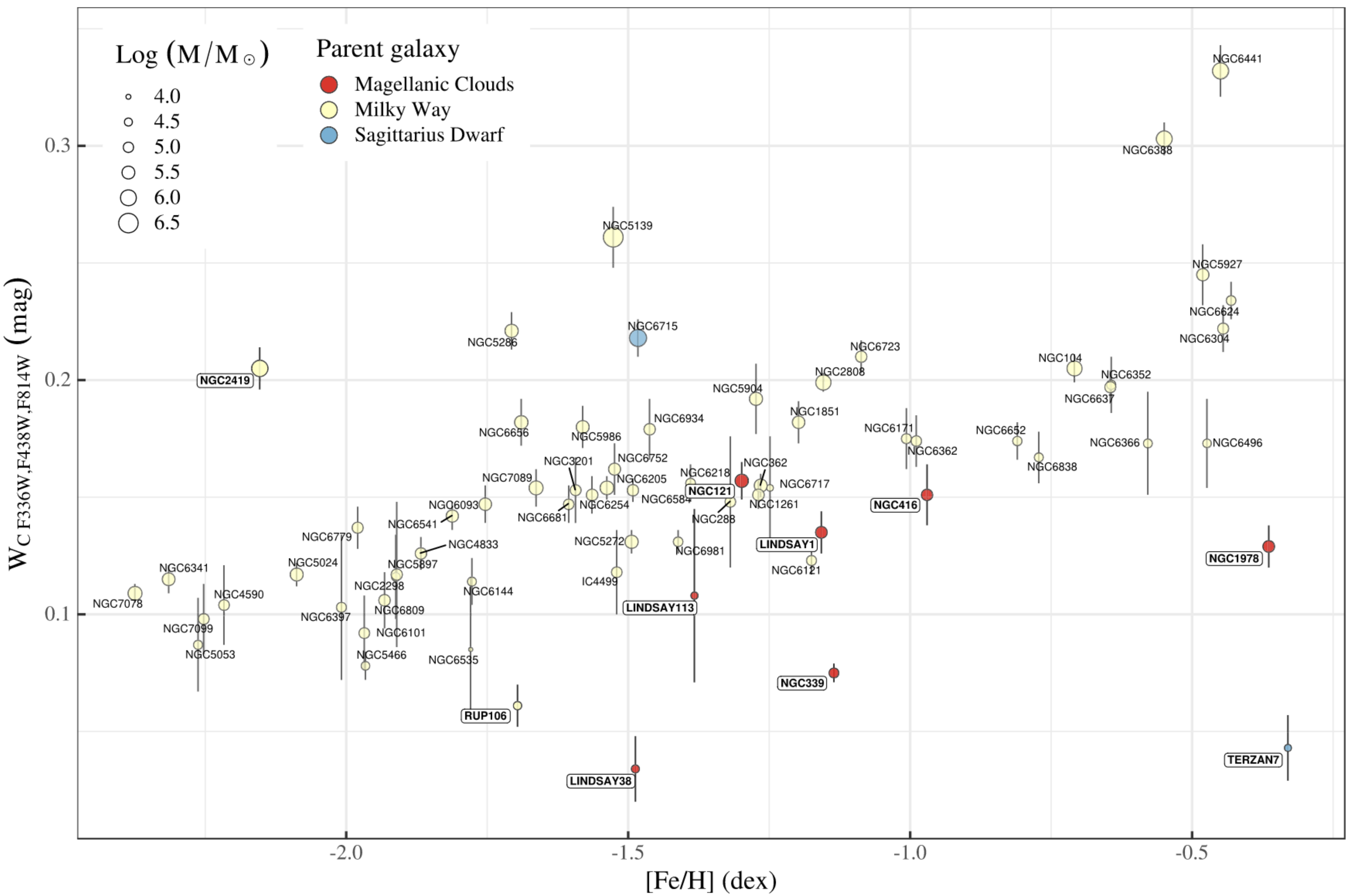

Log (M/M☉)
4.0
4.5
5.0
5.5
6.0
6.5
Parent galaxy
Magellanic Clouds
Milky Way
Sagittarius Dwarf
W C F336W,F438W,F814W (mag)
[Fe/H] (dex)
0.1
0.2
0.3
-2.0
-1.5
-1.0
-0.5
NGC6441
NGC6388
NGC5139
NGC5927
NGC6624
NGC6304
NGC6715
NGC5286
NGC2419
NGC6723
NGC104
NGC6352
NGC6637
NGC2808
NGC5904
NGC1851
NGC6171
NGC6362
NGC6652
NGC6838
NGC6366
NGC6496
NGC6656
NGC5986
NGC6934
NGC6752
NGC3201
NGC7089
NGC6205
NGC6218
NGC362
NGC6717
NGC121
NGC6584
NGC6254
NGC6681
NGC6093
NGC6541
NGC288
NGC1261
NGC416
NGC6779
NGC4833
NGC5272
NGC6981
LINDSAY1
NGC6121
NGC1978
NGC5024
NGC5897
NGC6341
NGC7078
NGC4590
NGC2298
NGC6144
IC4499
LINDSAY113
NGC6809
NGC6397
NGC7099
NGC6101
NGC5053
NGC5466
NGC6535
NGC339
RUP106
TERZAN7
LINDSAY38

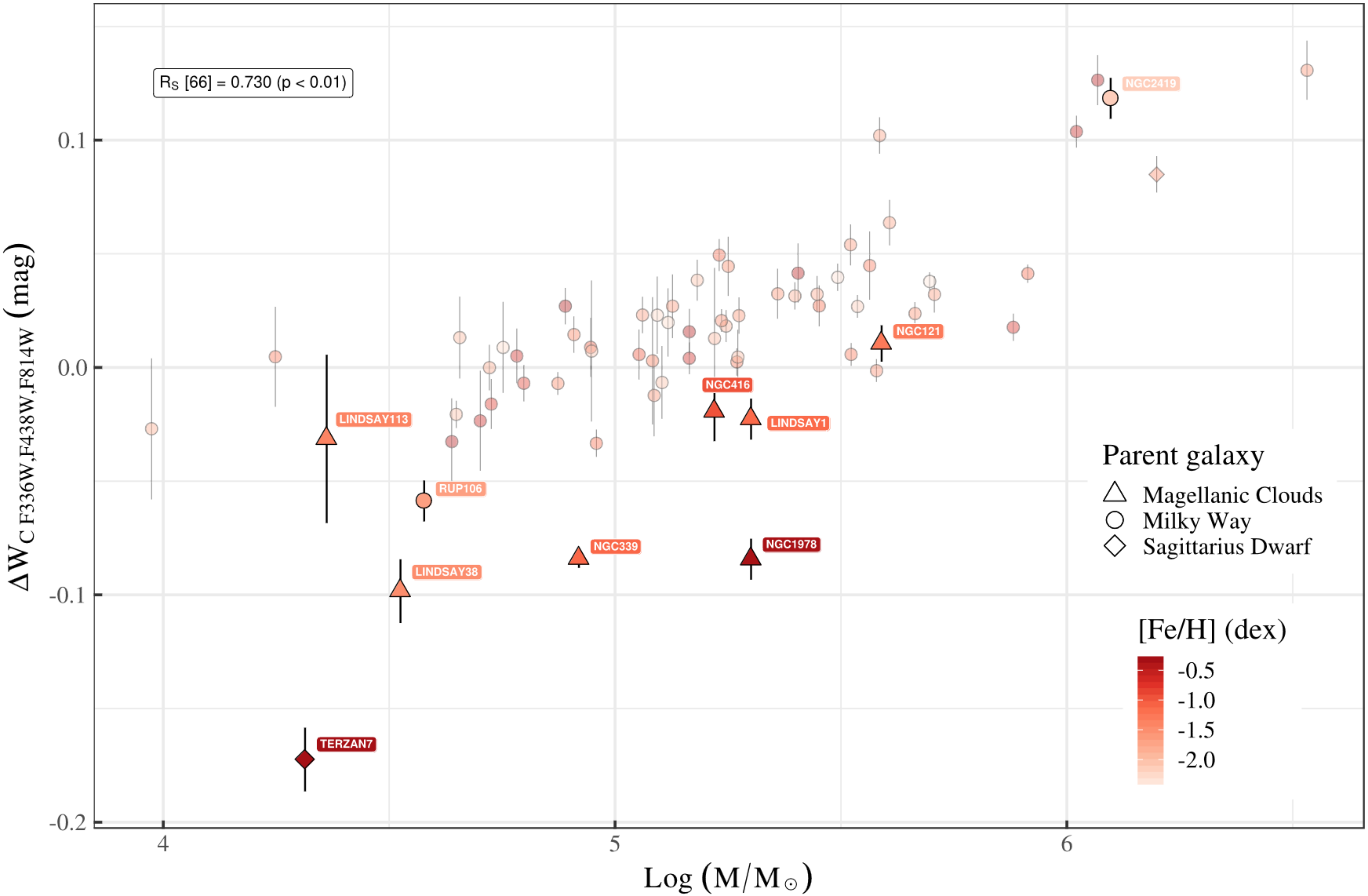

R_S [66] = 0.730 (p < 0.01)
NGC2419
LINDSAY113
RUP106
NGC416
LINDSAY1
NGC121
NGC339
NGC1978
LINDSAY38
TERZAN7
Parent galaxy
Magellanic Clouds
Milky Way
Sagittarius Dwarf
[Fe/H] (dex)
-0.5
-1.0
-1.5
-2.0
0.1
0.0
-0.1
-0.2
4
5
6
$\Delta W_{C\ F336W,F438W,F814W}$ (mag)
Log $(M/M_\odot)$

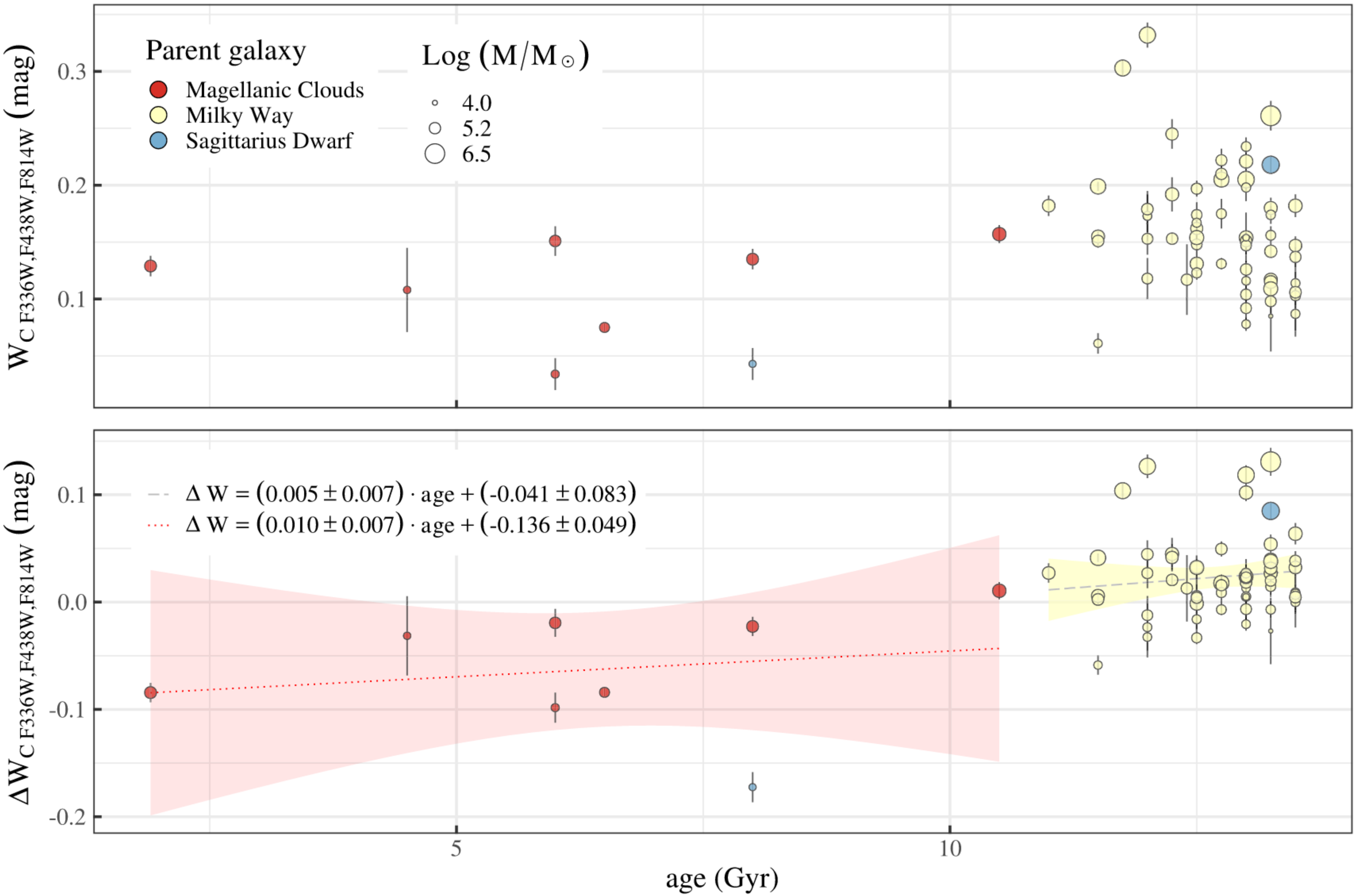

Parent galaxy
Magellanic Clouds
Milky Way
Sagittarius Dwarf
Log (M/M☉)
4.0
5.2
6.5
$W_{C\ F336W,F438W,F814W}$ (mag)
0.3
0.2
0.1
$\Delta W = (0.005 \pm 0.007) \cdot age + (-0.041 \pm 0.083)$
$\Delta W = (0.010 \pm 0.007) \cdot age + (-0.136 \pm 0.049)$
$\Delta W_{C\ F336W,F438W,F814W}$ (mag)
0.1
0.0
-0.1
-0.2
5
10
age (Gyr)

Conclusions

- for 68 GCs, measure of color extension of the stars at the base of the RGB in the UV–optical pseudocolor $C_{F336W,F438W,F814W}$ (sensitive to the stellar content of C, N, O, and helium)
- in the W $_{CF336W,F438W,F814W}$ versus [Fe/H], young and intermediate-age MC clusters and Terzan 7 attain systematically lower RGB width values with respect to the MW GCs
- Rup 106 (mono stellar population) -> Terzan 7 likely a single population cluster
- comparison between the normalized RGB width of the MW and extragalactic GCs as a function of the cluster mass demonstrates that the extragalactic GCs systematically deviate
- comparison between the bulk trend of the Galactic GCs and the extragalactic systems shows that the latter attaining lower values of $DW_{CF336W, F438W, F814W}$ -> MC GCs exhibit smaller internal light-element variations than Galactic GCs with similar present-day masses
- does the observed difference depend on specific physical conditions in Galactic and extragalactic proto-GCs at the epoch of formation? or do MPs in MW and extragalactic GCs follow a unique trend with the initial cluster mass, but ancient Galactic GCs lost significant amount of their mass?

zotero

Groups Documentation Forums Get Involved Log In Upgrade Storage

Your personal research assistant

Zotero is a free, easy-to-use tool to help you collect, organize, annotate, cite, and share research.

Download

Available for Mac, Windows, Linux, and iOS

Just need to create a quick bibliography? Try ZoteroBib.

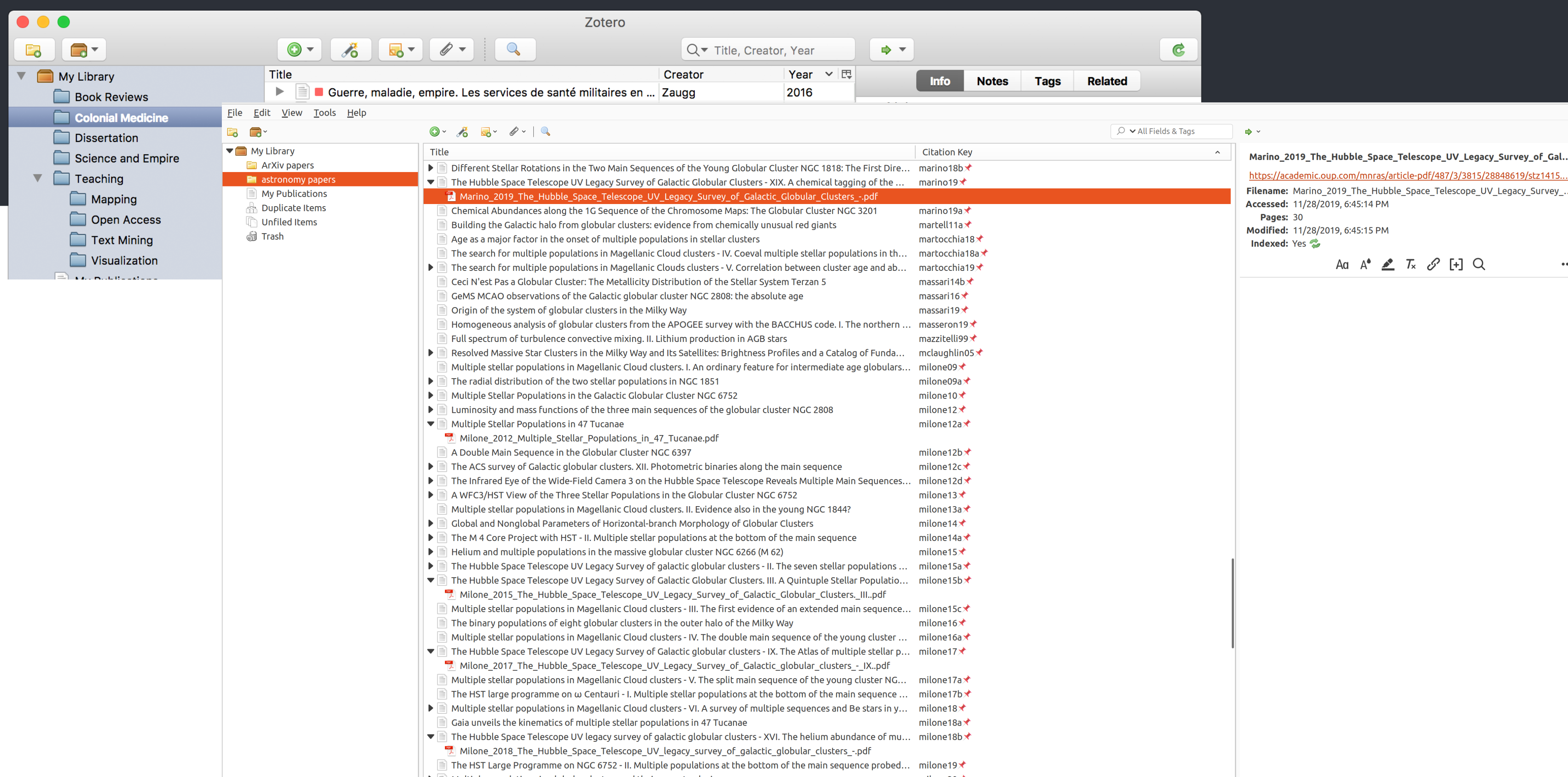

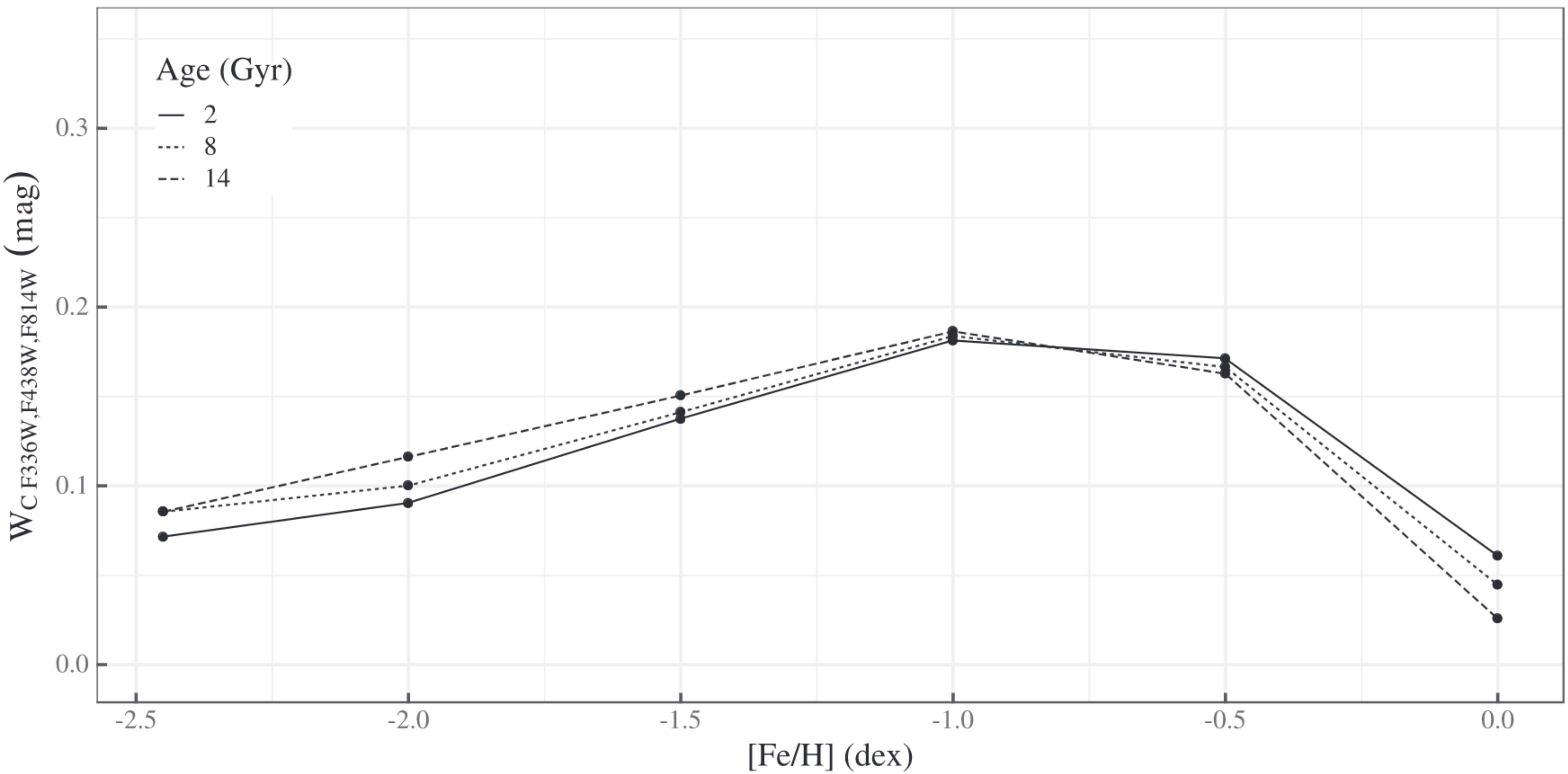

Figure 7. Theoretical variation of the RGB width as a function of metallicity [Fe/H] for young, intermediate-age, and old models.